

A MEMS Ultrasonic Transducer for Monitoring of Steel Structures

Akash Jain****^a, David W. Greve**^a, Irving J. Oppenheim*^{b+}

^aDepartment of Electrical and Computer Engineering

^bDepartment of Civil and Environmental Engineering, Carnegie Mellon University

ABSTRACT

Ultrasonic methods can be used to monitor crack propagation, weld failure, or section loss at critical locations in steel structures. However, ultrasonic inspection requires a skilled technician, and most commonly the signal obtained at the time of any inspection is not preserved for later use. A preferred technology would use a MEMS device permanently installed at a critical location, polled remotely, capable of on-chip signal processing that could exploit a signal history. We first review questions related to wave geometry, signal levels, flaw localization, and electromechanical design issues for microscale transducers. We then describe the design, characterization, and initial testing of a MEMS transducer to function as a detector array. The device is approximately 1-cm square and was fabricated by the MUMPS process. The chip has 23 sensor elements to function in a phased array geometry, each element containing 180 polysilicon diaphragms with a diameter of 85 microns and an unloaded natural frequency near 3.5 MHz. We report on characterization studies including capacitance-voltage measurements and admittance measurements. We then report on initial experiments, using a conventional piezoelectric transducer for excitation, with successful detection of signals in an on-axis transmission experiment, or the equivalent of a thickness-gauging application.

Keywords: Ultrasonics, MEMS, phased array, diaphragm, capacitive transducer

1. INTRODUCTION

Steel is the most important structural material used in buildings, bridges, pressure piping, and industrial construction; its properties of stiffness, strength, and ductility are, in many ways, ideal for those purposes. Aluminum alloys are the most important structural materials used in airframe construction for similar reasons. However, the continued safe performance of any such structure is threatened by section loss from corrosion or wear, crack propagation from fatigue or cyclic loading, weld failure from overload or seismic loading, and other discontinuities. These flaws develop with time, and the continued service of major structures typically requires confirmation that these flaws have not developed.

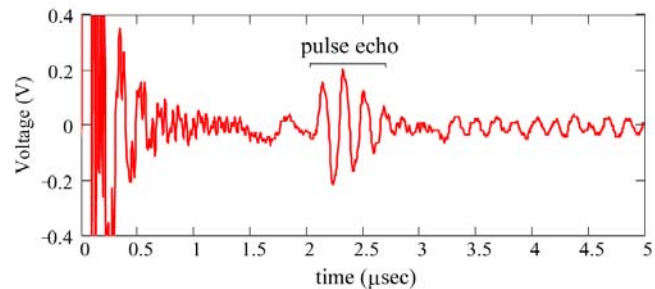
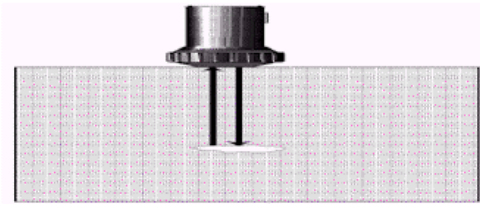


Figure 1a. Pulse-echo flaw detection (from ref [1])

Figure 1b. Results using mm-scale PZT specimen

Ultrasonic flaw detection¹ is a versatile technology for nondestructive evaluation, and must typically be performed by skilled personnel. The principles of pulse-echo flaw detection are depicted in Figures 1a and 1b for a through-thickness geometry. Figure 1a depicts an ultrasonic pulse generated and transmitted into the material. The transducer frequency is

⁺ * Contact author: ijo@cmu.edu; 412-268-2950; Carnegie Mellon University, Department of Civil and Environmental Engineering, Pittsburgh, PA 15213; ** dg07@andrew.cmu.edu; 412-268-3707; Department of Electrical and Computer Engineering; *** akash@andrew.cmu.edu.

typically between 1 and 10 MHz; higher frequencies have shorter wavelengths and thus are capable of detecting smaller flaws. For example, a 5 MHz frequency corresponds to a 1.2-mm wavelength in steel, a wavelength which is sufficiently short to resolve flaws at that scale. The typical transducer is a piezoelectric device, a PZT (lead-zirconium-titanate) ceramic, with a diameter of 15 mm. Because the transducer is many wavelengths in width, the wave is planar with little geometric spreading.

The pulse will reflect from the first boundary it encounters. In an unflawed specimen that boundary is the back surface of the steel plate, and the time at which the echo returns to the front surface reveals the total travel distance, equal to twice the thickness. Figure 1b records a measurement using a mm-scale PZT sample as a transducer affixed to an aluminum plate (velocity of sound $c = 6400$ m/s) with a thickness of 6.4 mm. The time from the pulse to the return of the echo is slightly in excess of $2 \mu\text{s}$, correctly reproducing the thickness. The mm-scale PZT specimen has dimensions comparable to the wavelength, and therefore the wave would be closer to spherical, with accompanying geometric spreading. In flaw detection, a flaw is revealed firstly by a premature echo, and the extent of the flaw is revealed from the operator's manual scan of the surface. The operator obtains additional information from the magnitude of the premature echo, which will vary with the geometry of the flaw surface. (These principles have been described for the simple case of a single transducer, normal incidence, and through-thickness geometry. Other inspection practices involve angled beams with multiple reflections across the thickness of the plate, separately positioned transducers for excitation and signal reception, and other specialized techniques which are not reviewed here.)

We note two limitations to current ultrasonic flaw detection practices: inspection is performed manually, and therefore subject to interpretation, and the process is often memoryless, taking no advantage of the earlier signal history. We envision building a resident ultrasonic flaw detection system to be mounted at critical locations on metal structures. The device would retain a signal history to allow signature analysis in the detection of developing flaws, and would be polled remotely using RF communications. This paper describes the design and initial testing of a MEMS capacitive (diaphragm-type) transducer array to function as the receiver in the flaw detection system, to operate in a phased array geometry.

2. PREVIOUS WORK

The principles of ultrasonic pulse-echo detection are used in many other applications including range/motion sensing, embedded object detection, surface characterization, and (perhaps most significantly) medical ultrasound imaging. For these reasons there is a considerable history of research into MEMS transducers for fluid-coupled and air-coupled applications. The investigators' approach to microscale ultrasonic diaphragm design was based on the important earlier work of Khuri-Yakub at Stanford University^{2,3,4,5,6}. One paper by Khuri-Yakub² outlines the mechanical and electrical analysis of capacitive diaphragm transducers and presents experimental results for air-coupled and fluid-coupled transmission through aluminum, showing that practical applications (including flaw detection) are feasible. Another³ records in detail the fabrication steps needed to produce capacitive ultrasonic transducers suitable for immersion applications and the characterization, both experimental and analytical, of their performance. Another⁴ presents results for nondestructive evaluation of metal specimens, in which air-coupled transducers generate and receive Lamb waves, which are useful for detecting near-surface flaws. Two other references^{5,6} discuss one-dimensional transducer arrays and present initial imaging results, in which solids immersed within fluids are detected. Other investigators of MEMS ultrasonics include Schindel^{7,8} with numerous contributions to immersion applications, and Eccardt^{9,10}, at Siemens, with the demonstration of surface micromachined transducers in a modified CMOS process.

3. TECHNICAL APPROACH

Figure 2 depicts a preliminary conceptual design of the intended system, at cm-scale, which evolved from a number of converging technical observations. MEMS capacitive (diaphragm-type) transducers are not effective at transmitting energy into a solid because the energy that can be developed in such a structure is small. Our conceptual design envisions a mm-scale PZT element to be made part of the packaging and to function as the pulse source. In our design the MEMS capacitive (diaphragm-type) transducers will operate in a phased-array geometry in order to localize signals

from the region around its fixed position, and MEMS fabrication is ideal for the manufacture of phased arrays. (Phased array implementations, with accompanying signal processing, permit imaging and off-axis sensing, and are used as such in medical ultrasound and in some small number of industrial applications.) An appropriate scale for the baseline of the phased array is a small multiple of the acoustic wavelength. An operating frequency near 3.5 MHz corresponds to a wavelength of approximately 2 mm and is a reasonable choice for purposes of flaw resolution, suggesting a baseline dimension on the order of 1 cm. Finally, the functions of system control, signal processing, data storage, power management, and RF communications for fly-by polling are envisioned in Figure 2 to reside in a CMOS electronics chip, although a single chip integrating the MEMS transducer array and the electronic circuits would be a desirable architecture for the device in the future.

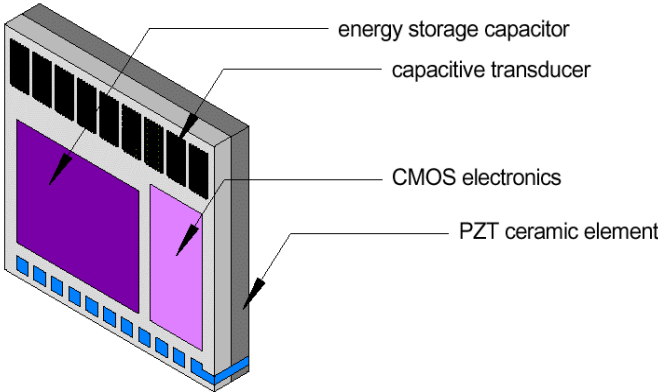


Figure 2. Conceptual design of integrated ultrasonic flaw detection device

4. DEVICE DESIGN

In a capacitive (diaphragm-type) transducer, diaphragm deflection produces a change in capacitance which can be detected electrically when a DC bias voltage is maintained across the plates of the capacitor. The sensitivity of any single diaphragm increases linearly with the bias voltage and inversely with the cube of the original (undeflected) gap dimension. Moreover, the sensitivity of any detector composed of diaphragms in parallel increases with the number of diaphragms, and therefore the most favorable utilization of area is preferred. Accordingly, a hexagonal plate geometry was chosen for the individual diaphragm unit, as pictured in Figure 3.

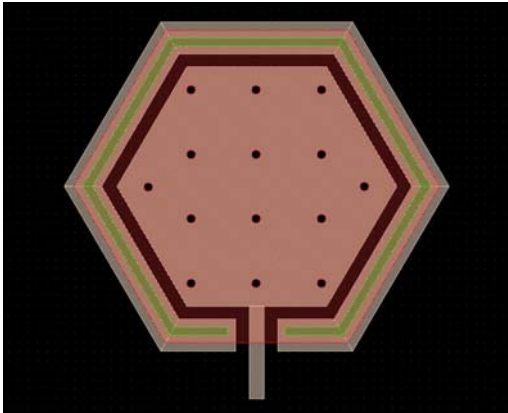


Figure 3. Typical diaphragm layout

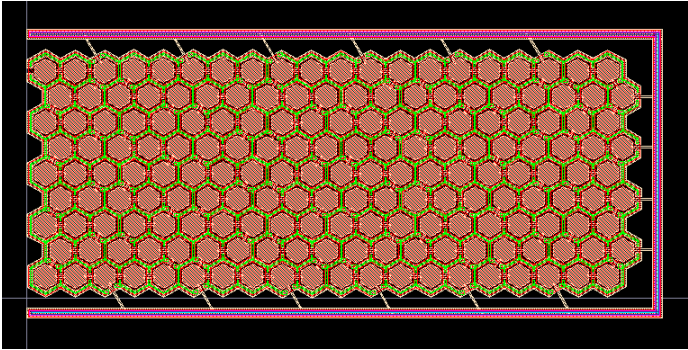


Figure 4. Typical detector

The MEMS diaphragm-type transducer was designed for fabrication by the MUMPS surface micromachining process, and Figure 3 is a mask layout drawing for the typical diaphragm. The diaphragm is constructed in the polysilicon-1 structural layer, with a thickness of 2 μm , and the holes are required per MUMPS design rules for the release etch of the sacrificial layer between the polysilicon-1 layer and the substrate. The diaphragm geometry is a regular hexagon and the length of each leg is equal to 49 μm , chosen to yield a resonant frequency near 4 MHz; a second diaphragm design was constructed on the same chip with a leg length equal to 69 μm . The elastic modulus for polysilicon is 180 GPa, the Poisson's ratio is 0.25, and the specific gravity is 2.300. Residual stress in the MUMPS polysilicon-1 layer is approximately 10 MPa compression, which is small compared to the calculated in-plane buckling stress

The underlying electrode area (not shown) is hexagonal with leg length equal to 37.5 μm , and the gap between the diaphragm and the electrode area on the substrate is 2 μm , from which the predicted capacitance for a single diaphragm is 0.016 pf. A target capacitance of a few pf was chosen, and therefore the basic detector was fabricated as a group of 180 diaphragms in parallel. Figure 4 is the layout drawing for a detector, with approximate dimensions of 0.5x2 mm.

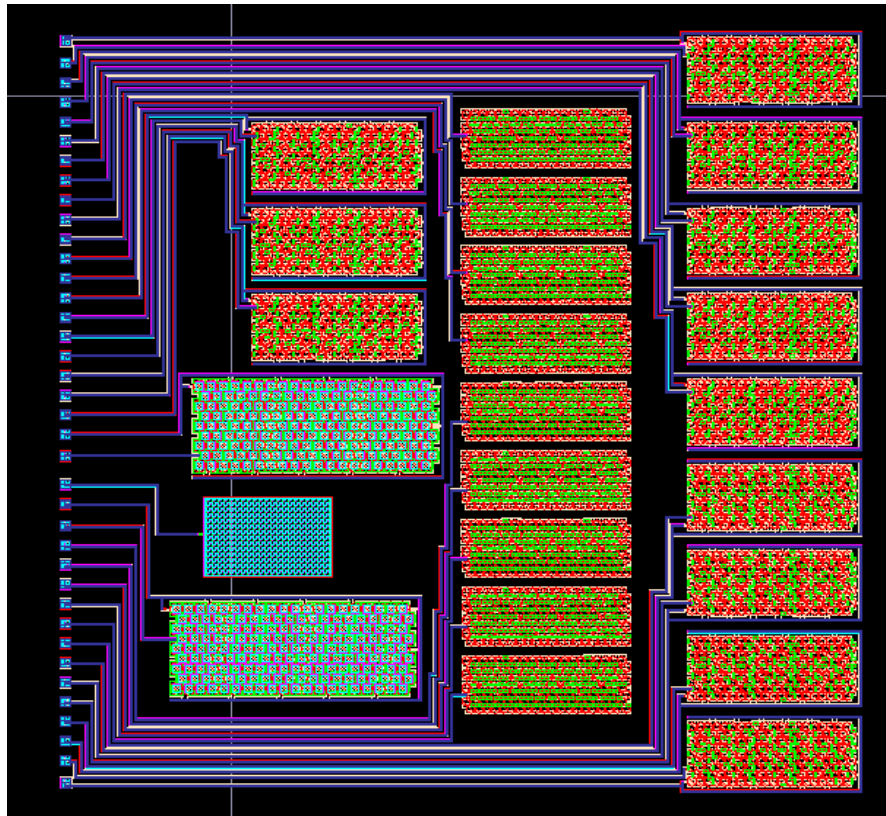


Figure 5. MEMS ultrasonic transducer array

The overall layout is shown in Figure 5 and is approximately 1-cm square, containing 23 detectors. The primary array is the set of nine detectors in the right-hand column, spanning a 1-cm baseline for phased array implementation. The nine detectors in the middle column are an unsuccessful alternate design attempting to use the substrate, rather than a deposited electrode surface, as the stationary plate of the capacitor. The three detectors at the top of the left-hand column constitute variations on the diaphragm design, using closer-spaced etch release holes, to perform experiments on squeeze film damping. The two largest detectors in the left-hand column are the alternate diaphragm designs constructed with two polysilicon layers, for a thickness of 4 μm , and a correspondingly larger leg dimension of 69 μm .

5. CHARACTERIZATION OF DEVICE PROPERTIES

Physical performance of a capacitive (diaphragm-type) transducer can be investigated experimentally by measuring capacitance C as a function of the applied DC bias voltage V . A bias voltage of either polarity will produce an attractive force between the plates, the diaphragm will deflect, and the capacitance will increase. In theory, the C-V relationship should be parabolic with the form $C(V) = C_0 + C_1V^2$, where C_0 is the capacitance of the undeflected device.

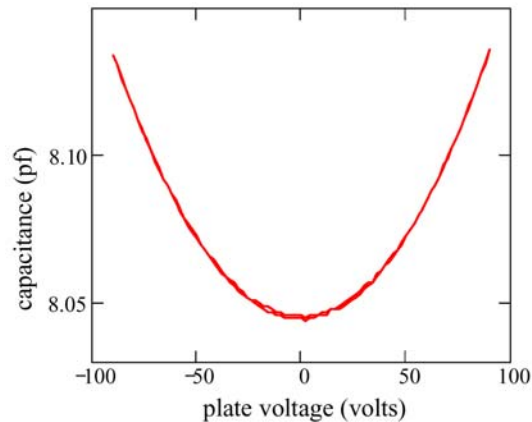


Figure 6. Experimental results, capacitance vs. voltage

Figure 6 shows typical experimental results obtained for the alternate diaphragm type, with $69\ \mu\text{m}$ leg length, and the measured C-V relationship is observed to be a parabola centered about zero voltage. The measured C-V relationship for the primary diaphragm type, with $49\ \mu\text{m}$ leg length, is not shown but was also a parabola as predicted. The C-V measurements were repeatable with no hysteresis.

Admittance measurements were conducted in vacuum for the primary diaphragm type, with $49\ \mu\text{m}$ leg length, and resonance was detected at 3.47 MHz. A natural frequency of 2.49 MHz is predicted for a simply-supported hexagonal plate with the dimensions of the subject diaphragm, whereas a natural frequency of 4.46 MHz is predicted for the case of fixed supports. It is common to assume fixed supports at the anchors of most MEMS structures, but the experimental results in this particular geometry suggest a support fixity intermediate between simply supported and perfectly clamped, as might be expected from structural precedents.

6. EXPERIMENTAL RESULTS AT SIGNAL DETECTION

The MEMS transducers were developed to study signal detection in direct contact with solids. Experiments were performed with chips bonded to aluminum specimens using a cyanoacrylate glue and to plexiglass specimens using Gelest Zipcone CG silicone adhesive. Commercial ultrasonic transducers, with rated operating frequencies of 3.5 MHz and 5 MHz, were used as the signal sources; these transducers, with nominal diameters of 15 mm, produce a high-energy planar wave.

The first study was a through-thickness transmission (thickness gauging) experiment on an aluminum plate with a thickness of 6.4 mm. Figure 7 shows experimental results establishing that the MEMS transducer can detect ultrasonic signals, suitable for flaw detection, in metal specimens. The MEMS transducer was placed in direct contact with the lower face of the aluminum plate, on-axis with a commercial transducer applied to the upper face. The experiment involved generating a pulse with the commercial transducer and determining if a signal could be detected by the MEMS transducer.

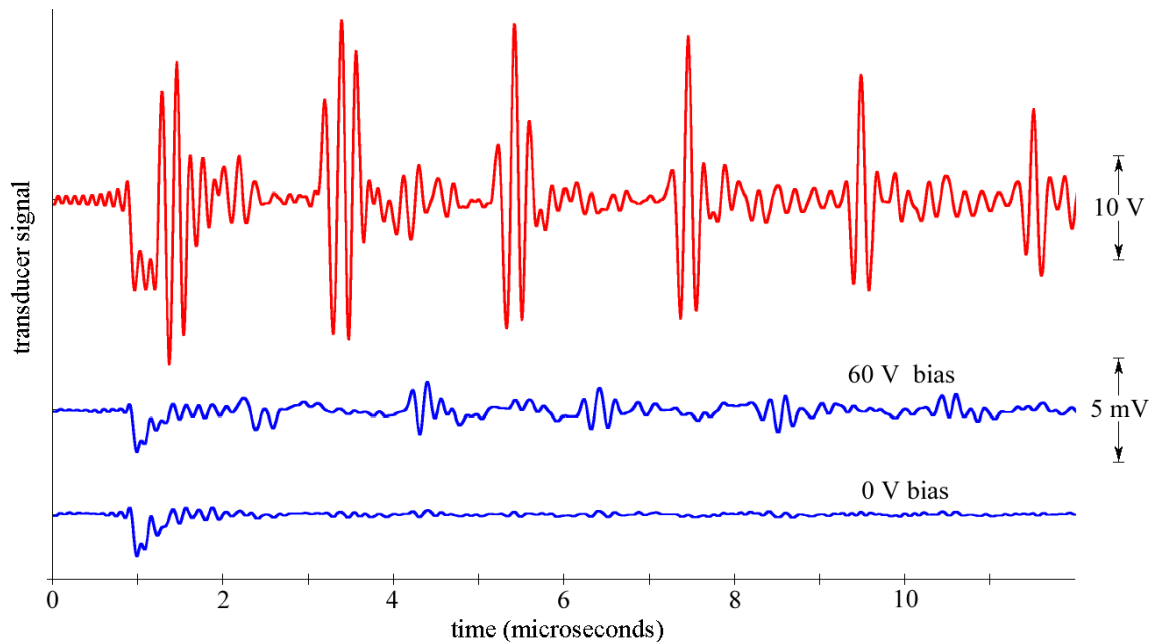


Figure 7. Through-thickness transmission experiments with MEMS transducer used as receiver

The upper plot in Figure 7 is the signal recorded from the commercial PZT transducer. It shows a pulse occurring at roughly $t = 1.2 \mu\text{s}$, followed by signals received at roughly $3.3 \mu\text{s}$, $5.4 \mu\text{s}$, and $7.5 \mu\text{s}$. (The pulse itself is attenuated in that record, but the subsequent signal is correctly shown in units of volts.) The time interval between the pulse and the first echo, roughly $2 \mu\text{s}$, equates to a travel distance of 12.8 mm , correctly corresponding to twice the specimen thickness. The wave continues to reflect from both surfaces, creating the repeating echoes observed every $2 \mu\text{s}$. The middle plot is the unamplified signal recorded from one detector on the MEMS transducer with an applied bias voltage equal to 60 V . There is a signal at the initial pulse time of $1.2 \mu\text{s}$ due to stray electrical coupling, and we then observe received signals at roughly $2.2 \mu\text{s}$, $4.3 \mu\text{s}$, and $6.2 \mu\text{s}$, in each instance at the midpoint of the intervals created by the echoes received at the upper face. The time interval between the pulse and the first signal, $1 \mu\text{s}$, equates to a travel distance of 6.4 mm , correctly corresponding to the specimen thickness. The ultrasonic pulse continues to reflect from both surfaces, creating the repeating echoes seen every $2 \mu\text{s}$ subsequently. The lower plot is an important control experiment, conducted at zero bias voltage, for which case no response should be observed. With the exception of the stray coupling at $1.2 \mu\text{s}$, the null result in the lower plot establishes that the signals recorded by the MEMS detector are not the result of stray coupling. Note that the commercial PZT transducer obtains signals greater by three orders of magnitude than the MEMS transducer.

The second study used a plexiglass specimen (velocity of sound $c = 2700 \text{ m/s}$) with non-parallel faces. Figure 8 depicts experimental results for a pulse illuminating the array of nine detectors from a distance of approximately 13 mm , oriented in a plane normal to the baseline. The following results are noted:

- The signal received at each detector is displayed on the plot at the relative spatial position of each detector. (Only eight signals are shown, because a contact pad for one detector became non-operative in the long course of the experiments.)
- Each signal shows the pulse near $1 \mu\text{s}$ because of stray electrical coupling, followed by the signal arrival approximately $4.5 \mu\text{s}$ later, corresponding roughly to the specimen thickness along that travel path.
- As predicted, the arrival time is uniform at all detectors.
- The signals at each detector are relatively uniform in appearance and comparable in amplitude.

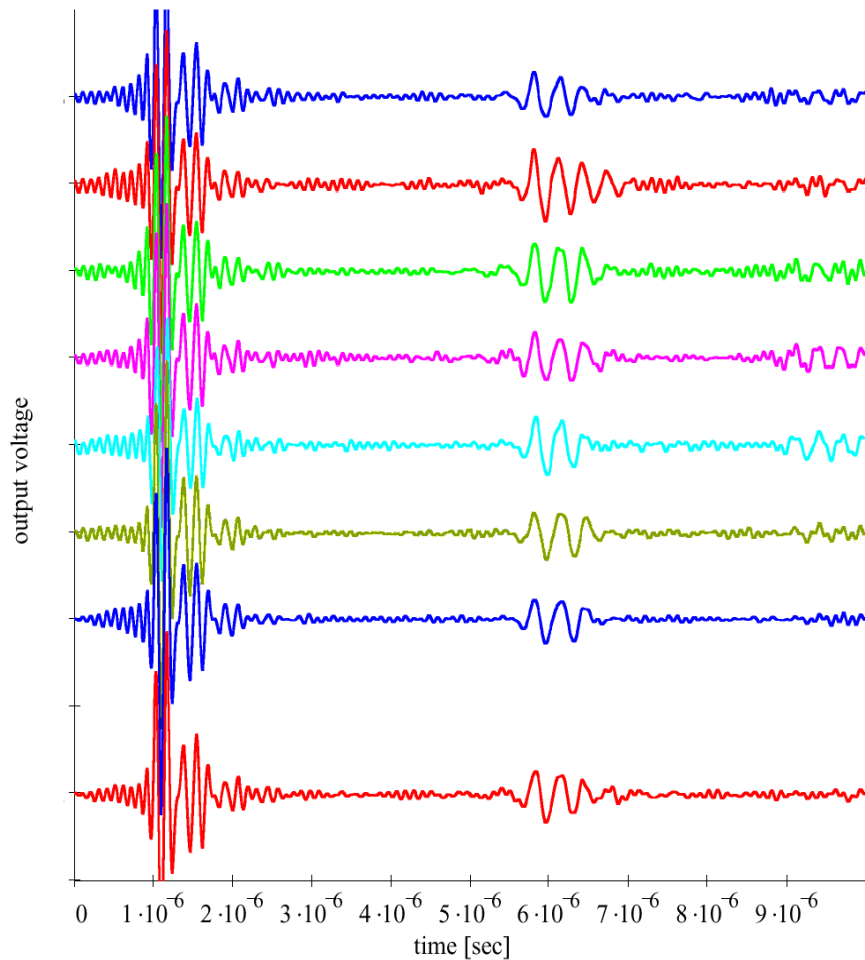


Figure 8. Experimental results, MEMS array response, uniform incidence

The third study featured a pulse originating along the axis of the baseline but 65° from the normal, arriving in a raking geometry from a point to the “north” of the array shown in Figure 5, positioned approximately 20 mm from the central detector of the array. Figure 9 depicts the experimental results, discussed as follows:

- Only seven detectors are shown, because the contact pads for two detectors became non-operative during the long course of the experiments.
- As expected, the signal arrives first at the closest detector, with successive delay in its arrival at each subsequent detector.
- The arrival times are consistent with the distance between the pulse source and the center of the array.
- The delay permits localization of the source, using the principles of radar imaging.
- A simple geometric localization can be envisioned directly on Figure 9. If a vertical line is drawn through the start of the pulses, and another straight line is drawn through the start of the received signals, those lines will intersect at a distanced which can be scaled (from the inter-detector spacing or the whole baseline dimension) to obtain the pulse origin to the “north” of the array.
- A mathematically simple reconstruction can be achieved by transforming each signal by a uniform delay in order to collocate them maximally. Figure 10 depicts the results of that process, with arbitrary units. The peaks along one axis represent the stray-coupled pulses, and should be deleted, while the remaining peak correctly shows the angle of incidence on that same axis and the distance from the array to the source on the other axis.

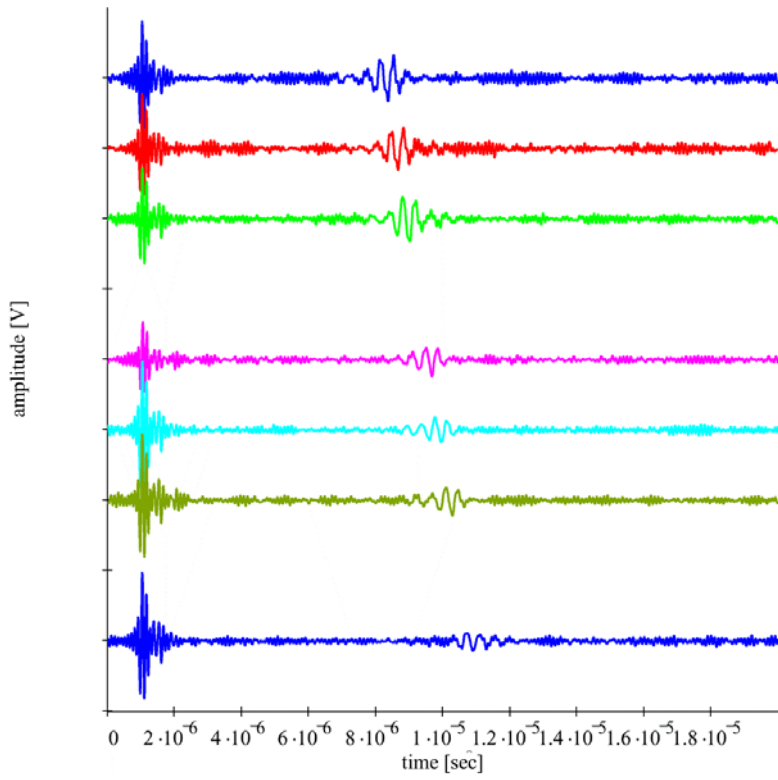


Figure 9. Experimental results, MEMS phased array response, off-axis incidence

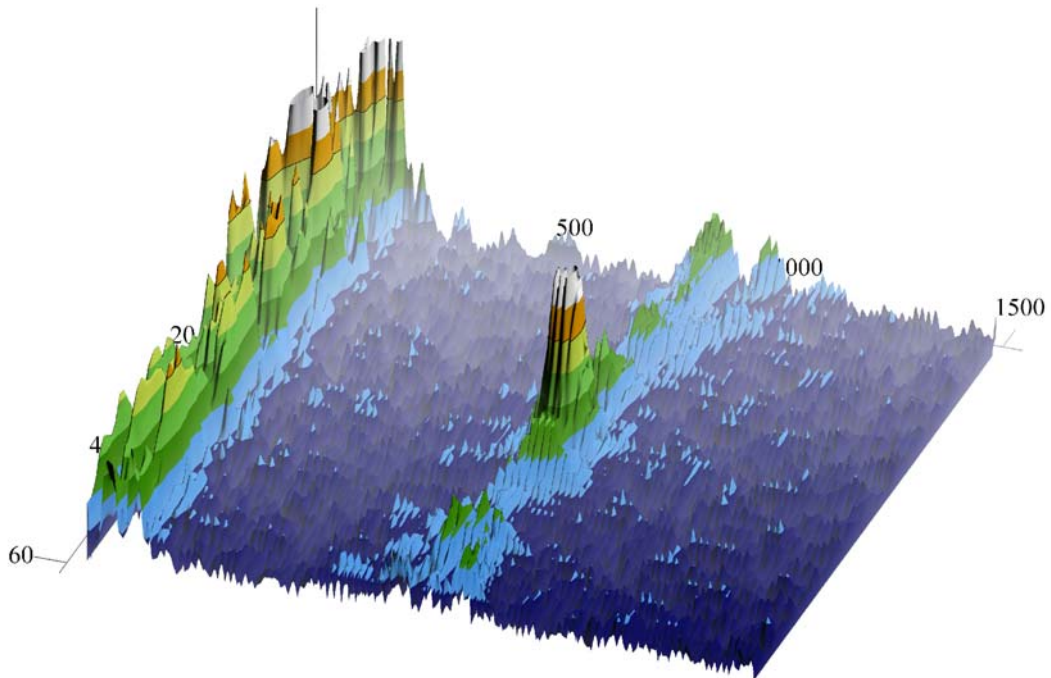


Figure 10. Collocation method of signal processing obtaining distance and orientation angle to source

7. CONCLUSIONS

Experimental results in Figures 7 through 9 show that MEMS capacitive (diaphragm-type) transducers can successfully detect ultrasonic pulses when fixed into contact with solids. A phased array implementation, Figures 9 and 10, shows that the transducer can successfully localize sources from off-axis geometries.

This first-generation device was designed to test the feasibility of phased array detection, to evaluate design alternatives, and to conduct related experiments in diaphragm behavior. Although the detectors fabricated in this first device are sufficiently sensitive to detect pulses from a commercial PZT transducer, improved sensitivity will be needed to detect pulses from mm-scale PZT sources. At present the sensitivity is limited by the capacitor gap and the detector area, and detection limits are seriously constrained by parasitic capacitances. A second-generation device is presently being fabricated with a number of design improvements to these conditions, and is expected to improve performance by an order of magnitude. Additional improvements in effective sensitivity, by orders of magnitude, can be achieved when the mechanical transducer and the electronic circuits are fabricated as an integrated system on a single chip.

ACKNOWLEDGEMENTS

This work has been funded by the Commonwealth of Pennsylvania through the Pennsylvania Infrastructure Technology Alliance program, administered at Carnegie Mellon by the Institute for Complex Engineering Systems, and by gifts from Krautkramer Inc., and the authors gratefully acknowledge that support.

REFERENCES

1. Krautkramer, J. and Krautkramer, H., *Ultrasonic Testing of Materials*, 4th edition, Springer Verlag, Berlin, 1989.
2. Ladabaum, I., Jin, X., Soh, H., Atalar, A., and Khuri-Yakub, B., "Surface micromachined capacitive ultrasonic transducers," *IEEE Trans. On Ultrasonics, Ferroelectrics, and Frequency Control*, Vol. 45, 678-690, 1998.
3. Jin, X., Ladabaum, Degertkin, F., Calmes, S., and Khuri-Yakub, B., "Fabrication and characterization of surface micromachined capacitive ultrasonic immersion transducers," *IEEE Jnl. Of Microelectromechanical Systems*, Vol. 8, 100-114, 1999.
4. Hansen, S., Mossawir, B., Ergun, A., Degertkin, F., and Khuri-Yakub, B., "Air-coupled nondestructive evaluation using micromachined ultrasonic transducer," *IEEE Ultrasonics Symposium*, 1037-1040, 1999.
5. Oralkan, O., Jin, X., Kaviani, K., Ergun, A., Degertkin, F., Karaman, M., and Khuri-Yakub, B., "Initial pulse-echo imaging results with one-dimensional capacitive micromachined ultrasonic transducer arrays," *IEEE Ultrasonics Symposium*, 959-962, 2000.
6. Jin, X., Soh, H., Oralkan, O., Degertkin, F., and Khuri-Yakub, B., "Characterization of one-dimensional capacitive micromachined ultrasonic immersion transducer arrays," *IEEE Trans. On Ultrasonics, Ferroelectrics, and Frequency Control*, Vol. 48, 750-760, 2001.
7. Schindel, D., "Air-coupled generation and detection of ultrasonic bulk-waves in metals using micromachined capacitive transducers," *Ultrasonics*, Vol. 35, 179-181, 1995.
8. Bashford, A., Schindel, D., and Hutchins, D., "Micromachined ultrasonic capacitance transducers for immersion applications," *IEEE Trans. On Ultrasonics, Ferroelectrics, and Frequency Control*, Vol. 45, 367-375, 1998.
9. Eccardt, P., Niederer, K., Scheiter, T., and Hierold, C., "Surface micromachined ultrasound transducers in CMOS technology," *IEEE Ultrasonics Symposium*, 959-962, 1996.
10. Eccardt, P., Niederer, K., and Fischer, B., "Micromachined transducers for ultrasound applications," *IEEE Ultrasonics Symposium*, 1609-1618, 1996.